Changing Metabolic Signatures of Amino Acids and Lipids During the Prediabetic Period in a Pig Model With Impaired Incretin Function and Reduced β-Cell Mass

Simone Renner,[1] Werner Römisch-Margl,[2] Cornelia Prehn,[3] Stefan Krebs,[1] Jerzy Adamski,[3,4] Burkhard Göke,[5] Helmut Blum,[1] Karsten Suhre,[2,6,7] Adelbert A. Roscher,[8] and Eckhard Wolf[1]

Diabetes is generally diagnosed too late. Therefore, biomarkers indicating early stages of β-cell dysfunction and mass reduction would facilitate timely counteraction. Transgenic pigs expressing a dominant-negative glucose-dependent insulinotropic polypeptide receptor ($GIPR^{dn}$) reveal progressive deterioration of glucose control and reduction of β-cell mass, providing a unique opportunity to study metabolic changes during the prediabetic period. Plasma samples from intravenous glucose tolerance tests of 2.5- and 5-month-old $GIPR^{dn}$ transgenic and control animals were analyzed for 163 metabolites by targeted mass spectrometry. Analysis of variance revealed that 26 of 163 parameters were influenced by the interaction Genotype × Age ($P \leq 0.0001$) and thus are potential markers for progression within the prediabetic state. Among them, the concentrations of seven amino acids (Phe, Orn, Val, xLeu, His, Arg, and Tyr) were increased in 2.5-month-old but decreased in 5-month-old $GIPR^{dn}$ transgenic pigs versus controls. Furthermore, specific sphingomyelins, diacylglycerols, and ether phospholipids were decreased in plasma of 5-month-old $GIPR^{dn}$ transgenic pigs. Alterations in plasma metabolite concentrations were associated with liver transcriptome changes in relevant pathways. The concentrations of a number of plasma amino acids and lipids correlated significantly with β-cell mass of 5-month-old pigs. These metabolites represent candidate biomarkers of early phases of β-cell dysfunction and mass reduction.
***Diabetes* 61:2166–2175, 2012**

From the [1]Chair for Molecular Animal Breeding and Biotechnology, and Laboratory for Functional Genome Analysis, Gene Center, Ludwig-Maximilians-Universität München, Munich, Germany; the [2]Institute of Bioinformatics and Systems Biology, Helmholtz Zentrum München, German Research Center for Environmental Health, Neuherberg, Germany; the [3]Institute of Experimental Genetics, Genome Analysis Center, Helmholtz Zentrum München, German Research Center for Environmental Health, Neuherberg, Germany; the [4]Institute of Experimental Genetics, Life and Food Science Center Weihenstephan, Technische Universität München, Freising-Weihenstephan, Germany; the [5]Medical Clinic II, Klinikum Grosshadern, Ludwig-Maximilians-Universität München, Munich, Germany; the [6]Faculty of Biology, Ludwig-Maximilians-Universität München, Planegg-Martinsried, Germany; the [7]Department of Physiology and Biophysics, Weill Cornell Medical College in Qatar, Education City-Qatar Foundation, Doha, Qatar; and the [8]Children's Research Center, Dr. von Hauner Children's Hospital, Ludwig-Maximilians-Universität München, Munich, Germany.
Corresponding author: Eckhard Wolf, ewolf@lmb.uni-muenchen.de.
Received 5 September 2011 and accepted 21 February 2012.
DOI: 10.2337/db11-1133
This article contains Supplementary Data online at http://diabetes.diabetesjournals.org/lookup/suppl/doi:10.2337/db11-1133/-/DC1.

See accompanying commentary, p. 1925.

The incidence of diabetes and of impaired glucose tolerance, a prestage of type 2 diabetes, is rapidly increasing (1). Changes in insulin secretion, glucose homeostasis, and insulin sensitivity may occur many years before the clinical manifestation of diabetes (2).

While insulin resistance—mostly associated with obesity—often precedes the development of hyperglycemia, overt diabetes develops only with the onset of β-cell dysfunction (3). There is evidence that reductions in both the first and second phases of insulin release occur equally early, precede insulin resistance, and therefore may represent the primary risk factor predisposing individuals to type 2 diabetes (4). An experimental approach to this hypothesis requires an animal model with progressive β-cell dysfunction in the absence of confounding factors such as insulin resistance and obesity.

Transgenic pigs expressing a dominant-negative glucose-dependent insulinotropic polypeptide (GIP) receptor ($GIPR^{dn}$) develop normally but exhibit reduced insulinotropic action of GIP (5), which is typically seen in type 2 diabetic patients (6). In 2.5-month-old $GIPR^{dn}$ transgenic pigs, intravenous glucose tolerance, insulin secretion, and the total β-cell volume do not differ from controls (5). The only overt clue pointing to a prediabetic condition is reduced oral glucose tolerance with a distinct delay in insulin secretion. The insulinogenic index, a parameter of early insulin response (7), is reduced in 2.5-month-old $GIPR^{dn}$ transgenic pigs compared with controls (0.47 vs. 0.96; $P < 0.05$). With increasing age, the gradual loss of glucose control in $GIPR^{dn}$ transgenic pigs becomes more obvious. Aged 5 months $GIPR^{dn}$ transgenic pigs show a more pronounced reduction in oral glucose tolerance, a distinct reduction of the corresponding insulin secretion (insulinogenic index: 0.44 vs. 2.71 in controls; $P < 0.01$), a 35% reduced total β-cell mass, and a trend of reduced intravenous glucose tolerance (5).

Comprehensive metabolic profiling of biofluids has been proposed to obtain a deeper understanding of the pathogenesis of prediabetes and also for biomarker discovery (8). Metabolomic approaches depict metabolite homeostasis and the dynamic responses of cells or organisms to environmental challenge, genetic modifications, or disease (9). Because many metabolites are quite universal, the information content of metabolome data from animal studies can be rapidly transferred to human studies (e.g., for biomarker discovery) (10).

The progressive nature of changes in $GIPR^{dn}$ transgenic pigs, together with the opportunity to take serial blood

samples of sufficient volume from unrestrained animals, creates a unique model to screen for metabolomic footprints associated with early (2.5-month-old animals) and late (5-month-old animals) prediabetic stages. A targeted metabolomic approach was used to facilitate quantitative discrimination of phenotypes with high resolution (11).

Our study revealed characteristic changes in plasma concentrations of specific amino acids and lipids, signifying the changes in intermediary metabolism during progression within the prediabetic period.

RESEARCH DESIGN AND METHODS

Animal model. GIPR^{dn} transgenic pigs have been generated as described previously (5). GIPR^{dn} transgenic pigs and age-matched controls were studied at age 2.5 or 5 months. All animals were housed in single pens under controlled conditions and had free access to water. Animals were fed a commercial diet (Supplementary Table 1) once daily and were fasted for 18 h prior to the glucose tolerance tests (GTTs). Physiological data of GIPR^{dn} transgenic pigs and controls are summarized in Table 1.

Intravenous GTT and recovery of blood samples. Intravenous GTTs (IVGTTs) were accomplished as described previously (5). Blood was collected at −10, 0, 1, 3, 5, 10, 20, 30, 40, 60, and 90 min relative to the glucose load. Blood samples were placed on ice immediately after collection, centrifuged at 1,500*g* for 15 min, and plasma was stored at −80°C. Plasma glucose levels were determined using an AU 400 autoanalyzer (Olympus, Hamburg, Germany). Plasma insulin levels were measured using a porcine insulin radioimmunoassay kit (Millipore, Billerica, MA). The homeostasis model assessment (HOMA) of β-cell function index (HOMA-β) and HOMA of insulin resistance index (HOMA-IR) were calculated as previously described (12). The insulinogenic index was calculated as the ratio of the increment of plasma insulin (μU/mL) to glucose concentration (mg/dL) 30 min relative to the oral glucose load (7).

Targeted metabolomics. Metabolites were quantified at the Helmholtz Center Munich using the Absolute*IDQ* p150 Kit (Biocrates Life Sciences AG, Innsbruck, Austria) covering amino acids (14), hexoses (H), free carnitine (C0), acylcarnitines (40), glycerophosphocholines (92), and sphingolipids (15). Leu and Ile are summarized as xLeu. Absolute quantification of amino acids, acylcarnitines, and hexoses in the biological sample was achieved by reference to internal standards labeled with stable isotopes. The semiquantitative assessment of lipids was achieved by several nonlabeled internal standards in every group (13). Concentrations of metabolites are reported in μmol/L unless indicated otherwise.

Microarray analysis. Total RNA was isolated from shock-frozen liver tissue samples from 5-month-old male GIPR^{dn} transgenic and control animals ($n = 3$ per group) using a tissue homogenizer (Silent Crusher M, Heidolph Instruments, Schwabach, Germany) and the Trizol method. Hybridization probes were prepared using the WT Expression (Ambion, Austin, TX) and Terminal Labeling Kits (Affymetrix, Santa Clara, CA) according to the manufacturers' instructions. Labeled probes were hybridized to Affymetrix custom Gene ST arrays (SNOWBALLs520824F), which were scanned using an Affymetrix GeneChip Scanner 3000. Raw data were normalized using robust multiarray analysis (14), and the gene list was ranked by differential expression and screened for overrepresentation of Kyoto Encyclopedia of Genes and Genomes (KEGG) pathways using gene set enrichment analysis (GSEA) (15).

Statistical analysis. Metabolite data were statistically evaluated by ANOVA (Linear Mixed Models; PROC MIXED; SAS 8.2), taking the fixed effects of genotype (GT; transgenic, control), age (2.5 months, 5 months), time (relative to glucose application), and the interaction GT × Age, as well as the random effect of animal into account (16). To account for multiple testing, only P values ≤0.0001 were considered significant in the initial screening for significant effects. If specific hypotheses were tested, P values <0.05 were considered significant if not indicated otherwise. Correlation analyses were performed using PROC CORR (SAS 8.2).

RESULTS

Plasma amino acid concentrations change with age and progression within the prediabetic state. Of the 14 plasma amino acids quantified, 6 (His, Trp, Orn, Ser, Phe, and xLeu) were significantly influenced by age and 7 (Phe, Orn, Val, xLeu, His, Arg, and Tyr) by the interaction GT × Age (i.e., the effect of GT was different in younger vs. older animals). In addition, the plasma concentrations of 6 amino acids (Arg, Orn, Phe, Ser, Tyr, and xLeu) were significantly affected by time (Supplementary Table 2) (i.e., their concentrations changed during the course of the IVGTT) (Supplementary Fig. 1). To account for this fact, least squares means (LSMs) and SEs were calculated for GT × Age (Fig. 1). Consistently, the plasma concentrations of Phe, Orn, Val, xLeu, His, Arg, and Tyr were increased in 2.5-month-old but decreased in 5-month-old GIPR^{dn} transgenic pigs versus age-matched controls. The concentration of Trp was not different between the younger transgenic and control pigs but was significantly reduced in the older transgenic animals (Fig. 1).

To evaluate previously proposed hypotheses (17) of an increased turnover of glucogenic amino acids during prediabetic stages, the sum of the main glucogenic amino acids Ser + Gly was tested. While in 2.5-month-old animals

TABLE 1
Physiological characteristics of GIPR^{dn} transgenic pigs and controls

	Aged 2.5 months			Aged 5 months		
	Transgenic	Control	P	Transgenic	Control	P
n (male/female)	3/2	3/3		6/3	4/5	
Age (weeks)	10.69 ± 0.07	10.79 ± 0.52	0.266	21.24 ± 0.55	20.76 ± 0.35	0.775
Body weight (kg)	21.06 ± 1.58	19.72 ± 2.48	0.663	73.56 ± 3.63	72.41 ± 2.47	1.000
Fasting glucose (mg/dL)	83.1 ± 7.54	90.82 ± 5.85	0.214	85.63 ± 3.03	86.85 ± 3.02	0.516
Fasting insulin (μU/mL)	1.738 ± 0.30	2.50 ± 0.33	0.181	3.45 ± 0.60	4.25 ± 0.63	0.150
HOMA-IR	0.37 ± 0.09	0.58 ± 0.10	0.250	0.76 ± 0.15	0.93 ± 0.17	0.166
HOMA-β (%)	66.80 ± 33.49	40.82 ± 9.09	0.930	64.59 ± 15.60	67.15 ± 10.55	0.164
Insulinogenic index (μU/mL)/(mg/dL)	0.47 ± 0.04	0.96 ± 0.17	**<0.05**	0.44 ± 0.10	2.71 ± 1.24	**<0.01**
Oral GTT						
AUC glucose (−10 to 120 min)	24,028 ± 1,519	19,248 ± 1,402	**<0.05**	23,111 ± 1,206	18,503 ± 799	**<0.05**
AUC insulin (−10 to 120 min)	5,155 ± 763	5,698 ± 625	0.351	6,178 ± 724	13,526 ± 1,967	**<0.01**
AUC insulin (−10 to 45 min)	1,932 ± 187	2,783 ± 247	**<0.05**	1,715 ± 403	6,002 ± 1,531	**<0.01**
IVGTT						
AUC glucose (−10 to 90 min)	13,562 ± 359	14,315 ± 651	0.663	14,252 ± 1,262	12,733 ± 868	0.165
AUC insulin (−10 to 90 min)	1,135 ± 111	1,254 ± 269	0.664	1,634 ± 191	1,982 ± 243	0.106
Total pancreatic β-cell volume (mm^3)	201.9 ± 22.6	217.6 ± 29.8	0.843	789.2 ± 80.2	1,208.6 ± 84.8	**<0.05**

Analyses of age, body weight, fasting glucose, and insulin levels of 5-month-old GIPR^{dn} transgenic pigs (tg) and controls (wt) include 9 tg and 9 wt pigs, whereby 5/4 tg and 5/4 wt pigs have been used for oral GTT/IVGTT, respectively. P values <0.05 were considered significant (indicated in boldface type).

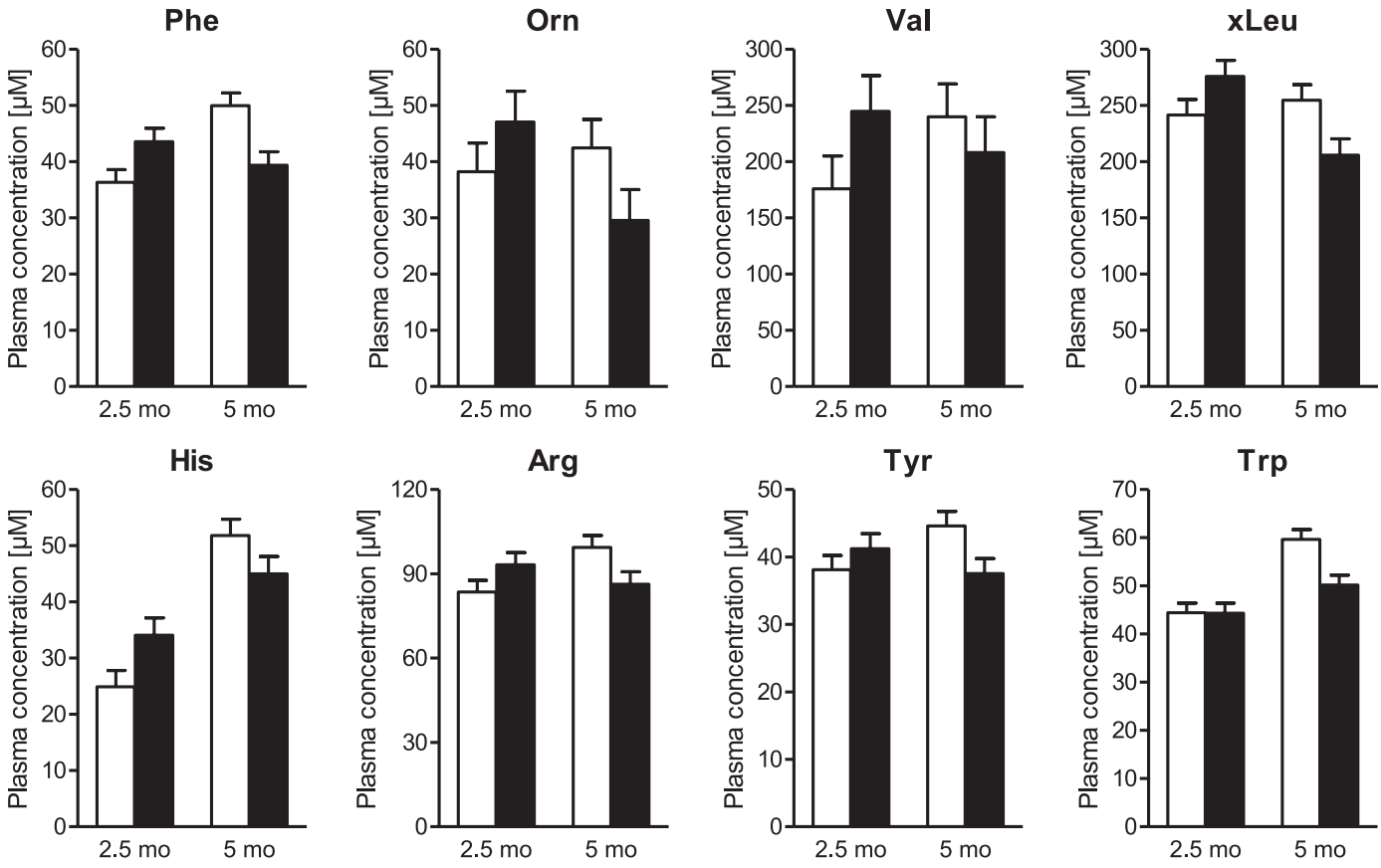

FIG. 1. Changes in plasma amino acid concentrations of 2.5- and 5-month-old GIPR^{dn} transgenic pigs (black columns) and controls (white columns) ordered according to the size of the GT × Age effect. LSMs and SEs calculated for GT (transgenic vs. control) × Age; all amino acid concentrations were significantly affected by the interaction GT × Age ($P < 0.0001$ for Phe, Orn, Val, xLeu, His, Arg, and Tyr; $P = 0.0003$ for Trp); $n = 4$ per GT and age class. mo, month.

there was no difference between the transgenic and the control group, 5-month-old transgenic pigs displayed a significantly reduced level of these glucogenic amino acids (LSM: 737 vs. 841 μmol/L in controls; GT × Age: $P = 0.0043$).

Amino acid profiling can potentially provide surrogate information on metabolic aberrations that may contribute to vascular endothelial dysfunction. Increase of reactive oxygen species, as observed in various diabetic conditions and models (18), may lead to consumption of tetrahydrobiopterin (BH4), the cofactor for the enzymes phenylalanine hydroxylase (EC 1.14.16.1) and nitric oxide synthase (EC 1.14.13.39). In addition, increased arginase activity has been reported in diabetic conditions and may contribute to vascular endothelial dysfunction by decreasing L-arginine availability to endothelial nitric oxide synthase (19). Potential aberrations in these enzymes were addressed by calculating Phe/Tyr and Orn/Arg ratios as indirect markers for phenylalanine hydroxylase and arginase activities. While both ratios were significantly affected by GT × Age ($P < 0.0001$), they did not reveal any sign of endothelial dysfunction in our model (not shown).

Plasma sphingomyelin concentrations are affected in GIPR^{dn} transgenic pigs. Different sphingolipid metabolites (e.g., ceramide) have been suggested to potentially be important regulators of β-cell survival, proliferation, and function (20,21). Since disturbed cellular sphingomyelin (SM) biosynthesis and metabolism might partially also be reflected in extracellular fluids, we included sphingomyelins in our screening panel. Sums of all SM (Fig. 2*A*) and hydroxysphingomyelin (SM-OH) (Fig. 2*B*) concentrations that have been measured (Supplementary Table 3) were calculated. In controls, circulating SM concentrations increased significantly with age ($P = 0.0002$); this increment was only marginal in GIPR^{dn} transgenic pigs (GT × Age: $P = 0.0393$). This was reflected by reduced concentrations of SM C24:0 (−17%), SM C24:1 (−9%), SM C16:0 (−15%), and SM C16:1 (−19%) in 5-month-old GIPR^{dn} transgenic pigs versus age-matched controls (Supplementary Table 3).

SM-OH concentrations were one order of magnitude lower than SM concentrations and were higher in 2.5-month-old

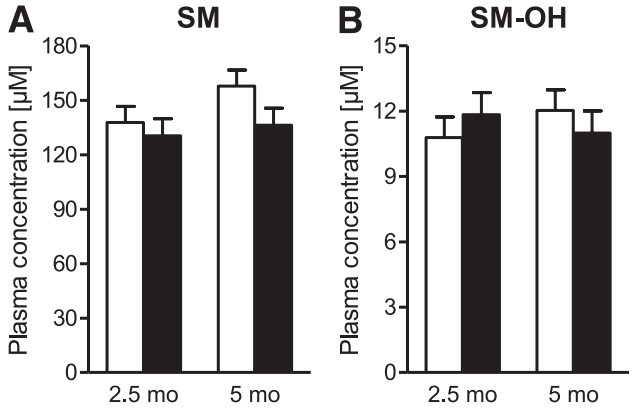

FIG. 2. Changes in the sum of SM (*A*) and SM-OH (*B*) concentrations in plasma from 2.5- and 5-month-old GIPR^{dn} transgenic pigs (black columns) and controls (white columns). LSMs and SEs calculated for GT × Age; *P* values for GT × Age are 0.0393 (SM) and 0.0004 (SM-OH). mo, month.

but lower in 5-month-old GIPR^{dn} transgenic pigs compared with age-matched controls (GT × Age: $P = 0.0004$). The concentrations of SM (OH) C22:1 (−18%) and SM (OH) C22:2 (−10%) were most prominently reduced in 5-month-old GIPR^{dn} transgenic pigs.

Altered concentrations of specific diacylglycerols, ether phospholipids, and lysophosphatidylcholines. Aberrant diacylglycerol levels have been reported in the context of prediabetes (22,23). Although the plasma level of PC aa C42:0 was increased in 2.5-month-old GIPR^{dn} transgenic pigs, decreased concentrations of PC aa C42:0, PC aa C42:4, and PC aa C42:5 were observed in 5-month-old transgenic animals when compared with age-matched controls (GT × Age: $P \leq 0.0001$) (Table 2). In addition, the plasma concentrations of a number of diacylglycerols were age dependent, with higher concentrations in 2.5- versus 5-month-old animals (Supplementary Table 4).

The plasma concentrations of several ether phospholipids were increased in 2.5-month-old GIPR^{dn} transgenic pigs, whereas decreased concentrations of specific ether phospholipids were measured in 5-month-old transgenic pigs compared with age-matched controls (GT × Age: $P \leq 0.0001$) (Table 2). In addition, a number of ether phospholipid concentrations were affected by age (Supplementary Table 5).

Specific plasma lysophosphatidylcholine concentrations were found to be decreased in 2.5-month-old (lysoPC a C16:1 and lysoPC a C20:3) or 5-month-old (lysoPC a C18:0) GIPR^{dn} transgenic pigs versus age-matched controls (GT × Age: $P \leq 0.0001$) (Table 2). A significant effect of age was observed for plasma concentrations of several lysophosphatidylcholines (Supplementary Table 6). The plasma concentration of lysoPC a C18:0 was significantly ($P < 0.0001$) affected by the intravenous glucose load (Supplementary Fig. 2*A*).

Altered concentrations of specific plasma acylcarnitines. Accumulation of plasma acylcarnitines was reported to be associated with absolute or relative insulin deficiency (24,25). Irrespective of age, the plasma concentration of glutaconyl-L-carnitine (C5:1-DC) was significantly increased in GIPR^{dn} transgenic pigs compared with controls (GT: $P < 0.0001$). In addition, a trend of increased levels of hydroxypropionyl-L-carnitine (C3-OH; GT: $P = 0.0003$), valeryl-L-carnitine (C5; GT: $P = 0.0036$), hexenoyl-L-carnitine (C6:1; GT: $P = 0.0006$), and octenoyl-L-carnitine (C8:1; GT: $P = 0.0018$) was detected in 2.5- and 5-month-old GIPR^{dn} transgenic pigs compared with age-matched controls (Supplementary Table 7). The plasma concentration of butyryl-L-carnitine (C4) was reduced in 2.5-month-old but increased in 5-month-old GIPR^{dn} transgenic pigs compared with controls (GT × Age: $P < 0.0001$). The plasma concentration of propionyl-L-carnitine (C3) was significantly influenced by age ($P < 0.0001$), with higher levels in 2.5- compared with

TABLE 2
Plasma diacylglycerol, ether phospholipid, and lysophosphatidylcholine concentrations (μmol/L) in GIPR^{dn} transgenic (tg) and wild-type (wt) pigs that are significantly influenced by GT × Age

		Aged 2.5 months			Aged 5 months			GT × Age	
Parameter	GT	LSM	SE	Δ (%)	LSM	SE	Δ (%)	*P* value	Age *P* value
PC aa C42:0	tg	0.1530	0.0115	**15.6**	0.1107	0.0115	**−16.7**	**0.0001**	0.0002
	wt	0.1324	0.0109		0.1329	0.0109			
PC aa C42:4	tg	0.1475	0.0166	−7.1	0.0920	0.0166	**−35.2**	**<0.0001**	**<0.0001**
	wt	0.1587	0.0153		0.1419	0.0153			
PC aa C42:5	tg	0.3068	0.0431	−0.6	0.1364	0.0431	**−40.1**	**<0.0001**	**<0.0001**
	wt	0.3086	0.0395		0.2279	0.0395			
PC ae C34:0	tg	0.6663	0.0569	**13.7**	0.4884	0.0569	**−12.5**	**<0.0001**	**<0.0001**
	wt	0.5858	0.0527		0.5582	0.0527			
PC ae C38:1	tg	0.9486	0.0976	**38.8**	0.6565	0.0976	−5.8	**<0.0001**	0.0003
	wt	0.6834	0.0915		0.6972	0.0915			
PC ae C38:2	tg	1.2434	0.1589	**29.7**	0.9914	0.1589	0.1	**<0.0001**	0.0011
	wt	0.9586	0.1463		0.9837	0.1463			
PC ae C40:3	tg	0.5575	0.0504	**26.0**	0.4036	0.0504	**−28.0**	**<0.0001**	0.4834
	wt	0.4424	0.0480		0.5604	0.0480			
PC ae C40:4	tg	1.9263	0.2291	**16.3**	1.4963	0.2291	**−10.4**	**0.0001**	0.0003
	wt	1.6566	0.2115		1.6691	0.2115			
PC ae C42:0	tg	0.4187	0.0288	7.4	0.3121	0.0288	**−11.4**	**<0.0001**	**<0.0001**
	wt	0.3899	0.0266		0.3521	0.0266			
PC ae C42:4	tg	0.1889	0.0195	5.7	0.1567	0.0195	**−32.6**	**<0.0001**	0.2012
	wt	0.1787	0.0184		0.2324	0.0184			
PC ae C42:5	tg	0.6791	0.0497	5.5	0.5943	0.0497	**−10.8**	**<0.0001**	0.0123
	wt	0.6438	0.0459		0.6665	0.0459			
PC ae C44:5	tg	0.1764	0.0133	1.7	0.1545	0.0133	**−28.0**	**<0.0001**	0.0547
	wt	0.1735	0.0125		0.2147	0.0125			
lysoPC a C16:1	tg	0.8792	0.1030	**−24.1**	0.9604	0.1030	−2.0	**<0.0001**	0.2802
	wt	1.1179	0.0950		0.9821	0.0950			
lysoPC a C18:0	tg	13.6348	1.2911	−9.3	16.5439	1.2911	**−21.6**	**<0.0001**	**<0.0001**
	wt	15.0459	1.1981		21.0933	1.1981			
lysoPC a C20:3	tg	0.4781	0.0931	**−38.5**	0.7126	0.0931	−11.3	**<0.0001**	**<0.0001**
	wt	0.7761	0.0856		0.8002	0.0856			

To account for multiple testing, only *P* values ≤0.0001 were considered significant (indicated in boldface type). Δ (%) = (tg – wt)/wt × 100; significant differences are indicated in boldface type. The full dataset of diacylglycerols, ether phospholipids, and lysophosphatidylcholines is provided in Supplementary Tables 4–6.

5-month-old animals. In addition, there was a trend of higher C3 levels in 2.5-month-old GIPR^{dn} transgenic pigs versus age-matched controls, while this difference was not present in the 5-month age-group (GT × Age: $P = 0.0010$). The plasma concentration of decanoyl-L-carnitine (C10) was significantly influenced by the glucose infusion during the IVGTT (Supplementary Fig. 2*B*).

Altered metabolite concentrations as a result of intravenous glucose infusion versus long-term changes. The differential metabolite profiles observed in our study could arise as the result of acute glucose challenge (intravenous glucose infusion) or might represent chronic alterations in glucose metabolism within the prediabetic state. To differentiate between these possibilities, the data analysis was restricted to a subset of metabolites and time points. Only the parameters that were significantly influenced by the interaction GT × Age and only the values from fasted plasma samples (10 min and 0 min before glucose infusion) were taken into account.

It is important that a significant effect of the interaction GT × Age was confirmed for 16 out of 26 metabolites, including all metabolite classes except acylcarnitines. This observation suggests that a significant proportion of the metabolite changes observed in our study are indicative of a chronic alteration of glucose metabolism, rendering them promising candidate biomarkers to monitor the prediabetic period. These metabolites are summarized in Table 3.

Glucose tolerance, insulin secretion, and total β-cell volume are correlated to specific plasma metabolite concentrations. Correlations were calculated by using data from the 5-month-old animals, since GIPR^{dn} transgenic pigs exhibited a 35% reduction in total β-cell volume at this stage. Metabolic parameters listed in Table 3 were included in the analysis, and all of those depicted in Fig. 3 correlated positively with total β-cell volume. Furthermore, Arg and the majority of plasma lipids selected correlated positively with parameters of insulin release. A negative correlation was revealed between lysoPC a C18:0 and, less clearly, PC ae C40:3, PC aa C42:4, and Val and area under the curve (AUC) glucose, in particular with AUC glucose (10–60).

Changes in liver transcriptome profiles are consistent with plasma metabolite changes. To evaluate if some of the plasma metabolite alterations were accompanied by expression changes of targets in corresponding metabolic pathways, we performed a holistic transcriptome study of liver samples from the three male GIPR^{dn} transgenic pigs and the three control boars in the 5-month age-group. GSEA was used as a tool, enabling sensitive detection of gene expression

TABLE 3
Fasting plasma metabolite concentrations (μmol/L) in GIPR^{dn} transgenic (tg) and wild-type (wt) pigs that are significantly influenced by GT × Age

		Aged 2.5 months			Aged 5 months			GT × Age	
Parameter	GT	LSM	SE	Δ (%)	LSM	SE	Δ (%)	*P* value	Age *P* value
Arg	tg	107.86	6.41	**20.2**	86.90	6.41	**−20.9**	**0.0009**	0.9403
	wt	89.70	6.35		109.87	6.35			
His	tg	37.19	3.78	**46.3**	45.12	3.78	**−22.4**	**0.0007**	**<0.0001**
	wt	25.42	3.75		58.12	3.75			
Phe	tg	48.73	3.24	**24.7**	38.06	3.24	**−30.3**	**<0.0001**	0.2929
	wt	39.08	3.17		54.62	3.17			
Val	tg	267.77	34.89	**46.5**	216.95	34.89	−18.7	**0.0001**	0.2589
	wt	182.77	32.79		266.84	32.79			
xLeu	tg	313.57	21.94	**20.3**	202.29	21.94	**−29.9**	**0.0006**	0.0231
	wt	260.57	21.64		288.60	21.64			
PC aa C42:0	tg	0.1659	0.0109	19.4	0.0886	0.0109	**−38.0**	**0.0012**	**0.0028**
	wt	0.1390	0.0109		0.1430	0.0109			
PC aa C42:4	tg	0.1581	0.0145	−5.3	0.0792	0.0145	**−45.4**	**0.0018**	**<0.0001**
	wt	0.1669	0.0139		0.1451	0.0139			
PC aa C42:5	tg	0.3175	0.0391	−4.7	0.1124	0.0391	**−50.0**	**0.0026**	**<0.0001**
	wt	0.3330	0.0365		0.2248	0.0365			
PC ae C40:3	tg	0.6300	0.0534	**25.1**	0.3136	0.0434	**−47.1**	**0.0012**	0.0455
	wt	0.5037	0.0534		0.5928	0.0534			
PC ae C42:5	tg	0.7193	0.0459	8.0	0.5447	0.0459	**−20.7**	**0.0020**	0.0116
	wt	0.6660	0.0443		0.6873	0.0443			
PC ae C44:5	tg	0.1858	0.0136	6.5	0.1395	0.0136	**−36.2**	**0.0008**	0.9252
	wt	0.1745	0.0135		0.2187	0.0135			
lysoPC a C18:0	tg	13.08	1.38	−9.4	13.68	1.38	**−32.5**	**0.0012**	**0.0002**
	wt	14.43	1.31		20.27	1.31			
SM OH C22:1	tg	3.6893	0.3413	3.2	3.1933	0.3413	**−28.5**	**0.0018**	0.3124
	wt	3.5753	0.3276		4.4691	0.3276			
SM OH C22:2	tg	1.9865	0.1452	15.1	1.5705	0.1452	**−20.5**	**0.0004**	0.3021
	wt	1.7256	0.1388		1.9766	0.1388			
SM C24:0	tg	10.76	0.83	−2.6	9.53	0.83	**−27.7**	**0.0031**	0.3718
	wt	11.05	0.80		13.18	0.80			
SM C24:1	tg	18.80	1.46	7.4	16.74	1.46	**−20.8**	**0.0028**	0.3545
	wt	17.51	1.40		21.14	1.40			

Δ [%] = (tg – wt)/wt × 100; significant differences are indicated in boldface type. To account for multiple testing within each metabolite class, only effects with *P* values ≤0.006 (acylcarnitines), ≤0.002 (amino acids), ≤0.006 (diacylglycerols), ≤0.002 (ether lipids), ≤0.006 (lysophosphatidylcholines), and ≤0.004 (SMs) were considered significant (indicated in boldface type).

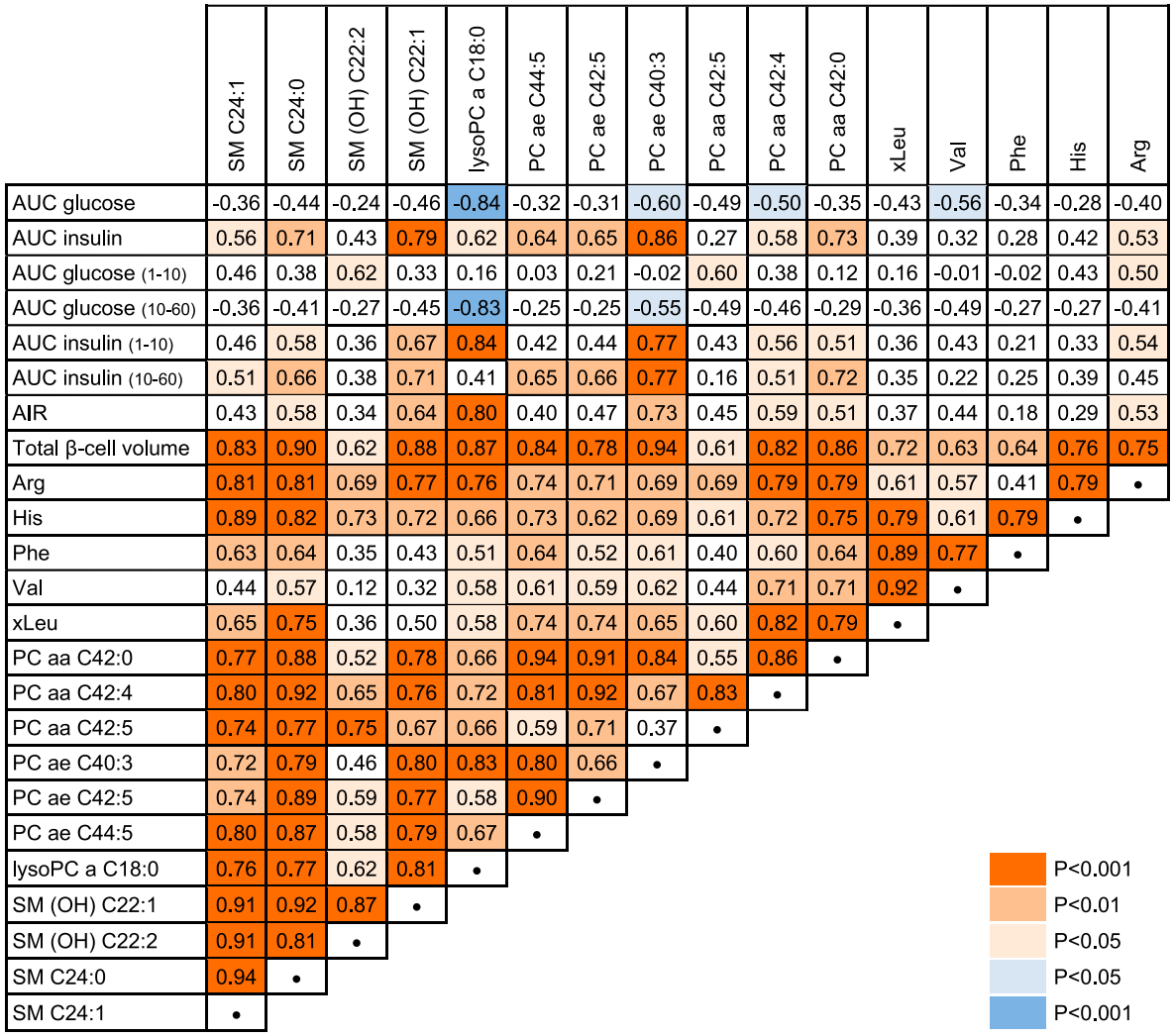

FIG. 3. Correlations between parameters of glucose tolerance and insulin secretion, total β-cell volume, and fasting plasma metabolite concentrations. AIR, acute insulin response (difference of mean plasma insulin at 1, 3, and 5 min after intravenous glucose load and fasting plasma insulin) (48).

changes within specific pathways (26). In accordance with several plasma metabolite alterations, GSEA indeed revealed liver transcript changes to be significantly enriched in a number of pathways already predicted by metabolite alterations. Those include Gly, Ser, and Thr metabolism, sphingolipid metabolism, and biosynthesis of unsaturated fatty acids (Table 4). A representative GSEA plot for genes involved in sphingolipid metabolism and the corresponding pathway with the observed transcriptome changes are shown in Fig. 4.

DISCUSSION

A number of targeted and nontargeted metabolomic studies have been performed to address metabolic correlates of clinically manifest diabetes (reviewed in Lucio et al. and Suhre et al.) (27,28). In addition, several studies performed metabolomic screens addressing classical risk factors, such as obesity, or pathogenetic mechanisms, such as insulin resistance. For instance, a monozygotic twin study screened for metabolomic correlates of acquired obesity and detected primarily increased levels of lysophosphatidylcholines, while ether phospholipids were decreased (29). Impaired insulin sensitivity in nondiabetic human subjects was found to be associated with altered metabolite profiles in lipid metabolic pathways, steroid hormone biosynthesis, and bile acid metabolism (27). Metabolomic profiling of obese versus lean humans revealed that serum concentrations of eight amino acids (Ala, Val, Leu/Ile, Phe, Tyr, Glu/Gln, Asp/Asn, and Arg) were markedly increased, while Gly was decreased, and defined a branched-chain amino acid (BCAA)-related metabolomic signature in obese subjects (30). A recent prospective study found the plasma concentrations of three BCAAs (Leu, Ile, and Val) and two aromatic amino acids (Phe and Tyr) to be significantly associated with the future risk of diabetes (31). However, the patients included in the latter study were characterized by an already increased BMI and HOMA-IR. Human subjects with even earlier stages of prediabetes characterized by β-cell dysfunction are only rarely diagnosed and, thus, difficult to recruit. Our genetically engineered pig model provides a unique time window to investigate the course of gradual β-cell mass reduction in relation to changes of intermediary metabolism. In contrast to human patients, the data on β-cell mass in pigs can also be obtained as quantitative information. A characteristic biochemical feature of this animal model

TABLE 4
Selected results of GSEA

KEGG pathway (ID)	Genes in the leading edge subset	NES	Nominal *P* value
Gly, Ser, and Thr metabolism (M766)	*SDS*, *PSPH*, *PIPOX*, *PHGDH*, *AOC2*, *CBS*, *ALAS2*, *GNMT*, *CTH*, *ALAS1*, *GATM*, *MAOA*, *AOC3*	1.45	0.053
Sphingolipid metabolism (M15955)	*ASAH2*, *UGT8*, *SGPP2*, *SGPL1*, *ACER3*, *DEGS2*	1.34	0.104
Glycosphingolipid biosynthesis—lacto and neolacto series (M17377)	*FUT2*, *B3GNT5*, *B3GALT5*, *ST3GAL4*, *GCNT2*, *B3GALT1*, *B3GALT2*, *ST3GAL6*, *FUT1*	−1.66	0.026
Pentose phosphate pathway (M1386)	*RPIA*, *ALDOC*, *PGM1*, *PGD*, *PGM2*, *PRPS2*, *PFKP*, *TKTL2*, *FBP2*	−1.66	0.024
Trp metabolism (M980)	*IL4I1*, *CYP1A1*, *ACMSD*, *AADAT*	−1.65	0.013
Biosynthesis of unsaturated fatty acids (M11673)	*ACOT4*, *ACOT7*, *HADHA*, *SCD*, *ELOVL2*, *YOD1*	−1.54	0.060
Lys degradation (M13720)	*EHMT1*, *HADHA*, *NSD1*, *TMLHE*, *PLOD1*, *AADAT*	−1.42	0.064
Amino sugar and nucleotide sugar metabolism (M8104)	*CYB5R1*, *PGM1*, *GNPDA2*, *GALK1*, *PGM2*, *UGDH*, *NANS*, *GNPNAT1*, *GFPT1*, *NAGK*, *GCK*, *PMM1*	−1.42	0.048

The enrichment score reflects the degree to which a set of genes belonging to a specific metabolic pathway is overrepresented at the extremes of the entire ranked list of differentially expressed genes. Adjustment for multiple hypothesis testing results in the normalized enrichment score (NES) (15). A positive NES indicates upregulation and a negative NES downregulation in the liver of GIPR^{dn} transgenic pigs. The gene lists are ordered according to their rank in the GSEA plot (see Fig. 4*A* as an example).

is the progressive reduction of the insulinogenic index with increasing life span. This parameter is correlated with impaired first-phase insulin release (7), which occurs in very early stages of β-cell dysfunction and is an important factor in the development of postprandial hyperglycemia (32).

Altered plasma amino acid concentrations as markers of prediabetes. Changes in plasma amino acid concentrations have been originally described in insulin-resistant obese patients (reviewed in Felig et al. and Muoio and Newgard) (33,34). In particular, elevated levels of BCAAs

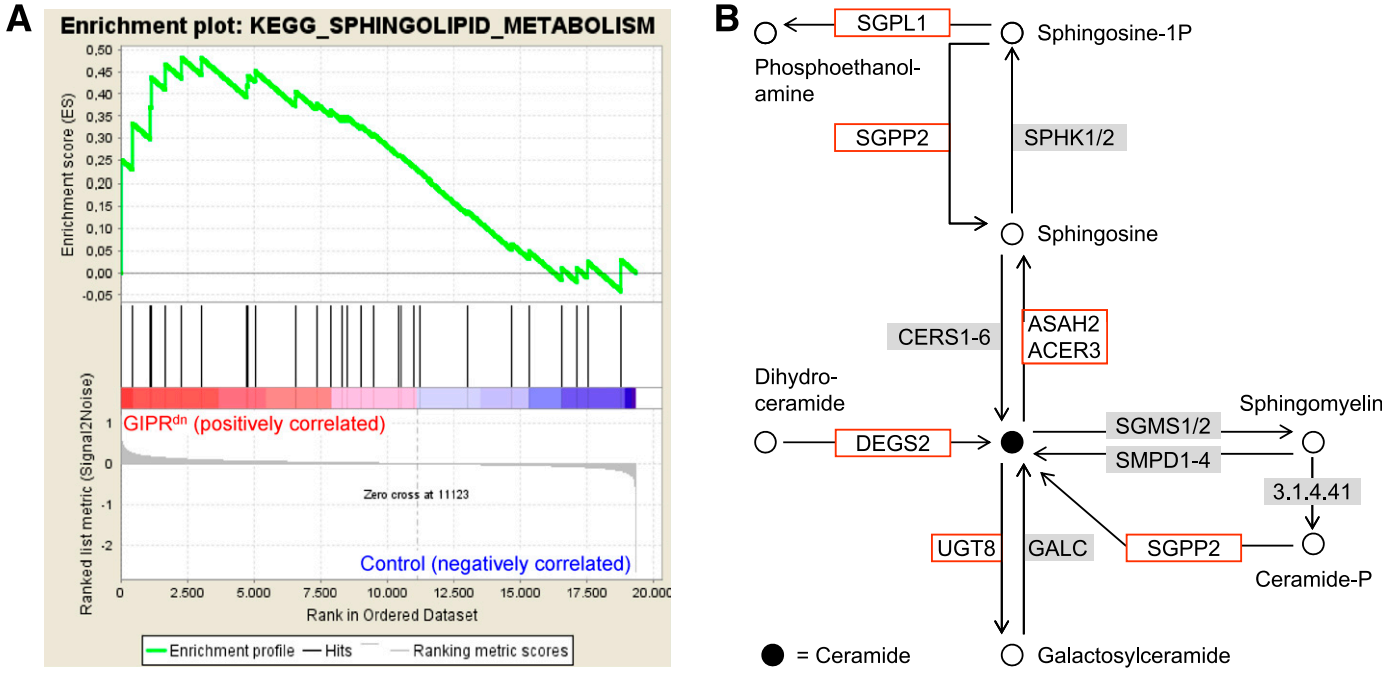

FIG. 4. GSEA revealed changes of sphingolipid metabolism in the liver of 5-month-old GIPR^{dn} transgenic pigs. *A*: Enrichment plot showing the distribution of genes of the KEGG pathway sphingolipid metabolism (vertical bars) in the list of genes expressed in liver samples ranked according to their differential expression between GIPR^{dn} transgenic and control pigs. The enrichment profile (green curve) shows a nonrandom distribution indicated by a roughly triangular outline and a peak close to one of the extremes of the signal-to-noise ordered dataset. This distribution means that a higher proportion of the pathway genes than expected under the null hypothesis are upregulated in GIPR^{dn} transgenic animals and fewer than expected are downregulated or neutral. The leading edge subset containing the most upregulated genes are the genes positioned left of the peak in the enrichment curve profile. These genes are listed in Table 4 and highlighted (red frame) in panel *B*. *B*: Partial sphingolipid metabolism pathway highlighting the products of genes that were upregulated in GIPR^{dn} transgenic pigs compared with controls and their enzymatic functions. The enzymes encoded by *ASAH2* and *UGT8*, which were the most upregulated genes of this pathway in GIPR^{dn} transgenic pigs, directly decrease the availability of ceramide, which is required for SM biosynthesis. Thus, the findings of the liver transcriptome analysis are in line with reduced plasma SM levels of 5-month-old GIPR^{dn} transgenic pigs. ACER3, alkaline ceramidase 3 (EC:3.5.1.23); ASAH2, N-acylsphingosine amidohydrolase (nonlysosomal ceramidase) 2 (EC:3.5.1.23); CERS1–6, ceramide synthase 1–6 (EC:2.3.1.24); DEGS2, sphingolipid delta-4 desaturase (EC:1.14.-.-); GALC, galactosylceramidase (EC:3.2.1.46); SGMS1/2, SM synthase 1/2 (EC:2.7.8.27); SGPL1, sphingosine-1-phosphate lyase 1 (EC:4.1.2.27); SGPP2, sphingosine-1-phosphate phosphatase 2 (EC:3.1.3.-); SMPD1–4, SM phosphodiesterase 1–4 (EC:3.1.4.12); SPHK1/2, sphingosine kinase 1/2 (EC:2.7.1.91); UGT8, UDP glycosyltransferase 8 (EC:2.4.1.45); EC 3.1.4.41, SM phosphodiesterase D.

have been confirmed in a number of subsequent studies of obese and/or insulin-resistant patient collectives (30,35,36) and in clinically manifest diabetes (28). Of interest, plasma levels of Val, Leu, Ile, Tyr, and Phe—known to be associated with diabetes risk in human subjects with increased BMI and reduced insulin sensitivity (31)—and those of Orn and Arg were elevated in 2.5-month-old GIPR^{dn} transgenic pigs, which show only a reduced incretin effect but are neither obese nor insulin resistant according to HOMA-IR (Table 1). This observation is remarkable because it demonstrates that a mild chronic disturbance of glucose homeostasis caused by reduced GIP function might be sufficient to result in a plasma amino acid profile suggestive for an increased risk to develop diabetes even in the absence of obesity. The elevated levels of seven amino acids in 2.5-month-old GIPR^{dn} transgenic pigs could be related to the distinct pattern of insulin secretion in this model. After an oral glucose load, initial insulin secretion is delayed, although the overall amount of insulin secreted during the 120-min period of the test reaches levels comparable with controls (5). In this respect, our model reflects the condition of impaired glucose tolerance preceding type 2 diabetes in human subjects where plasma insulin levels were reduced at 30 min after glucose ingestion but normal or increased at 120 min (37). The bell-shaped curve of insulin secretion in GIPR^{dn} transgenic pigs implicates a longer phase of insulin above a level that could inhibit gluconeogenesis and, thus, the use of glucogenic amino acids. A further possible explanation is that in comparison with the steep and fast increase of insulin secretion after oral glucose load, the slower increase in plasma insulin levels seen in GIPR^{dn} transgenic pigs could be a weaker anabolic signal, leading to less efficient amino acid uptake in peripheral tissues and clearance from the circulation (38,39).

It is surprising that initially elevated plasma levels of these amino acids (at 2.5 months) were reduced in 5-month-old GIPR^{dn} transgenic pigs, which show a more pronounced prediabetic phenotype (Table 1). The reduction in pancreatic β-cell mass and impaired insulin secretion after oral glucose load (5) and probably also after food intake might explain this effect. Of interest, the plasma concentrations of Arg, His, Phe, Val, and xLeu were correlated with total β-cell mass in 5-month-old pigs. During evolution toward diabetes, a continual mitigation of the inhibiting effect of insulin on hepatic gluconeogenesis would be expected to result in a higher demand and consumption of glucogenic amino acids. This hypothesis is indeed supported by the fact that the sum of the major glucogenic amino acids (Gly + Ser) was significantly reduced in plasma of 5-month-old GIPR^{dn} transgenic pigs. In addition, the liver transcriptome changes in 5-month-old pigs, showing enrichment of differentially expressed genes in corresponding pathways of amino acid metabolism, might also contribute to the observed alterations in plasma amino acid concentrations.

Specific amino acid ratios (Tyr to Phe and Orn to Arg) did not reveal signs of endothelial dysfunction as expected in view of our model. The GIPR^{dn} transgenic pig mimics different stages of the prediabetic period but is not yet manifesting with overt clinical signs.

Reduced levels of specific SMs are associated with impaired glucose homeostasis and moderately reduced β-cell mass. Sphingolipids are essential components of plasma membranes and endosomes and are critically involved in cell surface protection, protein and lipid transport and sorting, and cellular signaling cascades (40). Reduced plasma SM concentrations were recently observed in cynomolgus monkeys spontaneously developing hyperglycemia and hyperlipidemia (41).

We thus questioned if early stages of altered glucose homeostasis and β-cell dysfunction are associated with altered plasma concentrations of SM. It is interesting that GIPR^{dn} transgenic pigs did not show a comparable age-dependent increase in saturated SM species as observed in controls. In the more progressed prediabetic condition of 5-month-old GIPR^{dn} transgenic pigs, we found significant reductions in plasma levels of nearly all of the SM metabolites quantified (Supplementary Table 3). This observation is consistent with a recent study exploring specific sphingolipids as potential biomarkers in two different mouse models of insulin-dependent diabetes, streptozotocin-administered mice and *Ins2*^{Akita} mutant mice (42). In this study, plasma SM-C24:1 levels were consistently reduced in both models, and there was a trend of reduced SM C24:0 levels in the streptozotocin-administered animals. While both mouse models are characterized by a massive loss of β-cells, 5-month-old GIPR^{dn} transgenic pigs show only a modest disturbance of glucose homeostasis and a 35% reduction in β-cell mass. The concordance of SM changes in prediabetic GIPR^{dn} transgenic pigs with two mouse models with clinically manifest diabetes suggests that reductions in specific SMs could signify a proximal event in the cascade toward diabetes rather than being a consequence of manifesting disease. The fact that reduction of SM synthesis increases insulin sensitivity (43) raises the possibility that decreased SM levels in 5-month-old GIPR^{dn} transgenic pigs represent an adaptive response to reduced insulin secretion. It is interesting that there was a trend of a smaller HOMA-IR in 5-month-old GIPR^{dn} transgenic versus control pigs (see Table 1). The observed liver transcriptome changes related to SM metabolism (see Table 4 and Fig. 4) would support this concept. However, SM synthase 1 deficient mice show impaired insulin secretion (44). Thus, reduced SM levels, if present in β-cells, may also contribute to the impaired insulin secretion observed in 5-month-old GIPR^{dn} transgenic pigs.

Stage-specific changes in plasma phospholipid concentrations. Since plasma lipid profiles were found to be altered in obesity (29), an important risk factor for diabetes, we quantified the plasma concentrations of 38 diacylglycerols, 39 ether phospholipids, and 15 lysophosphatidylcholines in GIPR^{dn} transgenic and control pigs. While ether phospholipids can serve as endogenous antioxidants (45,46), increased levels of lysophosphatidylcholines have been described in the context of proinflammatory and proatherogenic conditions (reviewed in Pietiläinen et al.) (29). Acquired obesity was found to be associated with increases in lysophosphatidylcholines but decreases in ether phospholipids (29). Moreover, the levels of plasmalogens (ether lipids where the first position of glycerol binds a vinyl residue [from a vinyl alcohol] with the double bond next to the ether bond) were found to be decreased by ~50% in LDLs from type 2 diabetic patients (47).

Of interest is the finding that in 2.5-month-old GIPR^{dn} transgenic pigs, the concentrations of PC aa C42:0 and of several ether phospholipids were increased compared with age-matched controls. In contrast, decreased plasma concentrations of specific diacylglycerols and ether phospholipids were observed in 5-month-old GIPR^{dn} transgenic pigs. The latter may be interpreted as an early stage of loss of metabolic control associated with reduced antioxidant potential by ether phospholipids. Furthermore, as observed for the plasma amino acid concentrations, the reversed

plasma concentrations of some glycerophospholipids in 2.5- and 5-month-old GIPR^{dn} transgenic pigs are apparently indicative of progression within the prediabetic state.

Lysophosphatidylcholines were not elevated in GIPR^{dn} transgenic pigs. This is consistent with the fact that the metabolic alterations observed in 2.5- and 5-month-old GIPR^{dn} transgenic pigs are relatively mild and do not cause increased lipid peroxidation or other changes that might result in increased plasma lysophosphatidylcholine levels as observed in obesity and clinical diabetes (29).

Altered plasma acylcarnitine levels. Carnitine and its esters procure fatty acids for β-oxidation and therefore prevent fatty acid accumulation. Absolute or relative insulin deficiency results in increased and incomplete β-oxidation and accumulation of plasma acylcarnitines (24,25). In a recent study exploring metabolomic differences between obese and lean humans and their contribution to insulin resistance (30), 4 out of 37 acylcarnitine species measured were found to be increased in the plasma of obese subjects: propionyl-L-carnitine (C3), valeryl-L-carnitine (C5), hexenoyl-L-carnitine (C6), and octenoyl-L-carnitine (C8:1). Increased levels of short-chain acylcarnitines (C2, C6, and C8) also were observed in the diabetic state, and a positive correlation with plasma HbA_{1c} suggested a link with the severity of the disease (24). It is interesting that some short-chain acylcarnitines were also increased in GIPR^{dn} transgenic pigs, even at the age of 2.5 months. This observation indicates that in the absence of obesity, insulin resistance, or other severe disturbances of glucose homeostasis, short-chain acylcarnitines are sensitive parameters whose elevation suggests early stages and progression of prediabetes.

Candidate biomarkers for an early prediabetic state. Metabolite profiles of 2.5- and 5-month-old GIPR^{dn} transgenic pigs representing an early prediabetic state characterized by a reduced incretin effect and progressive reduction of glucose tolerance, insulin secretion, and pancreatic β-cell mass in part show similar changes as previously detected in obese, insulin-resistant, or diabetic patients. Thus, metabolite concentration alterations detected even in young GIPR^{dn} transgenic pigs appear to be sensitive indicators of very early stages of prediabetes. It is important that >50% of the metabolites altered in GIPR^{dn} transgenic pigs versus controls in an age- and disease progression–specific manner during an IVGTT were also detected if only fasting plasma samples were analyzed. Therefore, these parameters appear to be associated with long-term glucose control and do not arise only as the consequence of an intravenous glucose bolus. This observation also is important in practical terms because time-consuming GTTs are not essential. The age-dependent inverse alteration of specific plasma amino acid and lipid concentrations (elevated in 2.5-month-old and reduced in 5-month-old animals) going along with the progression of phenotypic changes in GIPR^{dn} transgenic pigs strongly argues for repeated metabolomic profiling in regular intervals, which is easily achievable in a large animal model. The fact that metabolic signatures observed in fasting plasma samples of 5-month-old GIPR^{dn} transgenic pigs were *1*) significantly correlated with total β-cell mass and *2*) associated with liver transcriptome changes in corresponding metabolic pathways support their potential usage as biomarkers.

In summary, our findings document the potential of a genetically designed large animal model resembling early stages of prediabetes in the absence of confounding obesity or insulin resistance for the discovery of candidate biomarkers that may serve as indicators of early stages of prediabetes.

ACKNOWLEDGMENTS

This study was supported by the Deutsche Forschungsgemeinschaft (GRK 1029), the Federal Ministry of Education and Research (Leading-Edge Cluster m^4–Personalized Medicine and Targeted Therapies), the Bayerische Forschungsstiftung (492/02), the Diabetes Hilfs- und Forschungsfonds Deutschland, a grant from the German Federal Ministry of Education and Research (BMBF) to the German Center Diabetes Research (DZD e.V.), BMBF Grant 03IS2061B (project Gani_Med), and BMBF Grant 0315494A (project SysMBo).

No potential conflicts of interest relevant to this article were reported.

S.R. researched data, contributed to discussion, and wrote, reviewed, and edited the manuscript. W.R.-M. and C.P. researched data, contributed to discussion, and reviewed and edited the manuscript. S.K. and H.B. performed the microarray study, including the bioinformatics analysis. J.A., B.G., and K.S. contributed to discussion and reviewed and edited the manuscript. A.A.R. and E.W. contributed to discussion and wrote, reviewed, and edited the manuscript. S.R. and E.W. are the guarantors of this work and, as such, had full access to all the data in the study and take responsibility for the integrity of the data and the accuracy of the data analysis.

The authors thank Julia Scarpa (Institute of Experimental Genetics, Genome Analysis Center, Helmholtz Zentrum München), Katharina Sckell (Institute of Experimental Genetics, Genome Analysis Center, Helmholtz Zentrum München), and Arsin Sabunchi (Institute of Bioinformatics and Systems Biology, Helmholtz Zentrum München) for metabolomics measurements performed at the Helmholtz Zentrum München, Genome Analysis Center, Metabolomics Core Facility.

REFERENCES

1. Hu FB. Globalization of diabetes: the role of diet, lifestyle, and genes. Diabetes Care 2011;34:1249–1257
2. Tabák AG, Jokela M, Akbaraly TN, Brunner EJ, Kivimäki M, Witte DR. Trajectories of glycaemia, insulin sensitivity, and insulin secretion before diagnosis of type 2 diabetes: an analysis from the Whitehall II study. Lancet 2009;373:2215–2221
3. Prentki M, Nolan CJ. Islet beta cell failure in type 2 diabetes. J Clin Invest 2006;116:1802–1812
4. Gerich JE. Is reduced first-phase insulin release the earliest detectable abnormality in individuals destined to develop type 2 diabetes? Diabetes 2002;51(Suppl. 1):S117–S121
5. Renner S, Fehlings C, Herbach N, et al. Glucose intolerance and reduced proliferation of pancreatic beta-cells in transgenic pigs with impaired glucose-dependent insulinotropic polypeptide function. Diabetes 2010;59:1228–1238
6. Nauck MA, Heimesaat MM, Orskov C, Holst JJ, Ebert R, Creutzfeldt W. Preserved incretin activity of glucagon-like peptide 1 [7-36 amide] but not of synthetic human gastric inhibitory polypeptide in patients with type-2 diabetes mellitus. J Clin Invest 1993;91:301–307
7. Kosaka K, Kuzuya T, Hagura R, Yoshinaga H. Insulin response to oral glucose load is consistently decreased in established non-insulin-dependent diabetes mellitus: the usefulness of decreased early insulin response as a predictor of non-insulin-dependent diabetes mellitus. Diabet Med 1996; 13(Suppl. 6):S109–S119
8. Bain JR, Stevens RD, Wenner BR, Ilkayeva O, Muoio DM, Newgard CB. Metabolomics applied to diabetes research: moving from information to knowledge. Diabetes 2009;58:2429–2443
9. Griffiths WJ, Wang Y. Mass spectrometry: from proteomics to metabolomics and lipidomics. Chem Soc Rev 2009;38:1882–1896
10. Koulman A, Lane GA, Harrison SJ, Volmer DA. From differentiating metabolites to biomarkers. Anal Bioanal Chem 2009;394:663–670
11. Griffiths WJ, Koal T, Wang Y, Kohl M, Enot DP, Deigner HP. Targeted metabolomics for biomarker discovery. Angew Chem Int Ed Engl 2010;49: 5426–5445
12. Wallace TM, Levy JC, Matthews DR. Use and abuse of HOMA modeling. Diabetes Care 2004;27:1487–1495

13. Römisch-Margl W, Prehn C, Bogumil R, Röhring C, Suhre K, Adamski J. Procedure for tissue sample preparation and metabolite extraction for high-throughput targeted metabolomics. Metabolomics 2012;8:133–142.
14. Irizarry RA, Bolstad BM, Collin F, Cope LM, Hobbs B, Speed TP. Summaries of Affymetrix GeneChip probe level data. Nucleic Acids Res 2003;31:e15
15. Subramanian A, Tamayo P, Mootha VK, et al. Gene set enrichment analysis: a knowledge-based approach for interpreting genome-wide expression profiles. Proc Natl Acad Sci U S A 2005;102:15545–15550
16. Verbeke G, Molenberghs G. *Linear Mixed Models for Longitudinal Data*. New York, Springer, 2001
17. Wijekoon EP, Skinner C, Brosnan ME, Brosnan JT. Amino acid metabolism in the Zucker diabetic fatty rat: effects of insulin resistance and of type 2 diabetes. Can J Physiol Pharmacol 2004;82:506–514
18. Pitocco D, Zaccardi F, Di Stasio E, et al. Oxidative stress, nitric oxide, and diabetes. Rev Diabet Stud 2010;7:15–25
19. Romero MJ, Platt DH, Tawfik HE, et al. Diabetes-induced coronary vascular dysfunction involves increased arginase activity. Circ Res 2008; 102:95–102
20. Sjöholm A. Ceramide inhibits pancreatic beta-cell insulin production and mitogenesis and mimics the actions of interleukin-1 beta. FEBS Lett 1995;367:283–286
21. Kelpe CL, Moore PC, Parazzoli SD, Wicksteed B, Rhodes CJ, Poitout V. Palmitate inhibition of insulin gene expression is mediated at the transcriptional level via ceramide synthesis. J Biol Chem 2003;278:30015–30021
22. Kumashiro N, Erion DM, Zhang D, et al. Cellular mechanism of insulin resistance in nonalcoholic fatty liver disease. Proc Natl Acad Sci U S A 2011;108:16381–16385
23. Timmers S, Schrauwen P, de Vogel J. Muscular diacylglycerol metabolism and insulin resistance. Physiol Behav 2008;94:242–251
24. Adams SH, Hoppel CL, Lok KH, et al. Plasma acylcarnitine profiles suggest incomplete long-chain fatty acid beta-oxidation and altered tricarboxylic acid cycle activity in type 2 diabetic African-American women. J Nutr 2009; 139:1073–1081
25. Steiber A, Kerner J, Hoppel CL. Carnitine: a nutritional, biosynthetic, and functional perspective. Mol Aspects Med 2004;25:455–473
26. Mootha VK, Lindgren CM, Eriksson KF, et al. PGC-1alpha-responsive genes involved in oxidative phosphorylation are coordinately downregulated in human diabetes. Nat Genet 2003;34:267–273
27. Lucio M, Fekete A, Weigert C, et al. Insulin sensitivity is reflected by characteristic metabolic fingerprints—a Fourier transform mass spectrometric non-targeted metabolomics approach. PLoS ONE 2010;5:e13317
28. Suhre K, Meisinger C, Döring A, et al. Metabolic footprint of diabetes: a multiplatform metabolomics study in an epidemiological setting. PLoS ONE 2010;5:e13953
29. Pietiläinen KH, Sysi-Aho M, Rissanen A, et al. Acquired obesity is associated with changes in the serum lipidomic profile independent of genetic effects—a monozygotic twin study. PLoS ONE 2007;2:e218
30. Newgard CB, An J, Bain JR, et al. A branched-chain amino acid-related metabolic signature that differentiates obese and lean humans and contributes to insulin resistance. Cell Metab 2009;9:311–326
31. Wang TJ, Larson MG, Vasan RS, et al. Metabolite profiles and the risk of developing diabetes. Nat Med 2011;17:448–453
32. Del Prato S, Marchetti P, Bonadonna RC. Phasic insulin release and metabolic regulation in type 2 diabetes. Diabetes 2002;51(Suppl. 1):S109–S116
33. Felig P, Marliss E, Cahill GF Jr. Plasma amino acid levels and insulin secretion in obesity. N Engl J Med 1969;281:811–816
34. Muoio DM, Newgard CB. Mechanisms of disease: molecular and metabolic mechanisms of insulin resistance and beta-cell failure in type 2 diabetes. Nat Rev Mol Cell Biol 2008;9:193–205
35. Pietiläinen KH, Naukkarinen J, Rissanen A, et al. Global transcript profiles of fat in monozygotic twins discordant for BMI: pathways behind acquired obesity. PLoS Med 2008;5:e51
36. Tai ES, Tan ML, Stevens RD, et al. Insulin resistance is associated with a metabolic profile of altered protein metabolism in Chinese and Asian-Indian men. Diabetologia 2010;53:757–767
37. Gerich JE. Metabolic abnormalities in impaired glucose tolerance. Metabolism 1997;46(Suppl. 1):40–43
38. Felig P. Amino acid metabolism in man. Annu Rev Biochem 1975;44: 933–955
39. Fukagawa NK, Minaker KL, Rowe JW, et al. Insulin-mediated reduction of whole body protein breakdown. Dose-response effects on leucine metabolism in postabsorptive men. J Clin Invest 1985;76:2306–2311
40. Pruett ST, Bushnev A, Hagedorn K, et al. Biodiversity of sphingoid bases ("sphingosines") and related amino alcohols. J Lipid Res 2008;49:1621–1639
41. Shui G, Stebbins JW, Lam BD, et al. Comparative plasma lipidome between human and cynomolgus monkey: are plasma polar lipids good biomarkers for diabetic monkeys? PLoS ONE 2011;6:e19731
42. Fox TE, Bewley MC, Unrath KA, et al. Circulating sphingolipid biomarkers in models of type 1 diabetes. J Lipid Res 2011;52:509–517
43. Li Z, Zhang H, Liu J, et al. Reducing plasma membrane sphingomyelin increases insulin sensitivity. Mol Cell Biol 2011;31:4205–4218
44. Yano M, Watanabe K, Yamamoto T, et al. Mitochondrial dysfunction and increased reactive oxygen species impair insulin secretion in sphingomyelin synthase 1-null mice. J Biol Chem 2011;286:3992–4002
45. Engelmann B. Plasmalogens: targets for oxidants and major lipophilic antioxidants. Biochem Soc Trans 2004;32:147–150
46. Zoeller RA, Lake AC, Nagan N, Gaposchkin DP, Legner MA, Lieberthal W. Plasmalogens as endogenous antioxidants: somatic cell mutants reveal the importance of the vinyl ether. Biochem J 1999;338:769–776
47. Colas R, Pruneta-Deloche V, Guichardant M, et al. Increased lipid peroxidation in LDL from type-2 diabetic patients. Lipids 2010;45:723–731
48. Marcelli-Tourvieille S, Hubert T, Pattou F, Vantyghem MC. Acute insulin response (AIR): review of protocols and clinical interest in islet transplantation. Diabetes Metab 2006;32:295–303